

Constrained Motion Approach to the Synchronization of the Multiple Coupled Slave Gyroscopes

Harshavardhan Mylapilli¹

Abstract: A set of n gyroscopes are coupled to form a system of slave gyroscopes. A simple approach is developed for synchronizing the motion of these slave gyroscopes whose individual motion may be regular or chaotic, with the motion of an independent master gyroscope irrespective of the chaotic or regular motion exhibited by the master. The problem of synchronization of these multiple gyroscopes is approached from a constrained motion perspective through the application of the fundamental equation of mechanics. The approach yields explicit, closed-form expressions for the control torques that are required to be applied to each of the coupled slave gyroscopes to achieve exact synchronization with the master's motion. The influence of different types of interactions between the slave gyroscopes is investigated with an incidence matrix that describes the coupling between any two of them. The effect of the so-called sleeping condition on the synchronization of the gyroscopes is also explored. To illustrate the efficacy of the methods presented in this paper, we consider numerical examples involving systems of multiple gyroscopes and synchronize them with the motion of a master gyroscope. DOI: [10.1061/\(ASCE\)AS.1943-5525.0000192](https://doi.org/10.1061/(ASCE)AS.1943-5525.0000192). © 2013 American Society of Civil Engineers.

CE Database subject headings: Control systems; Coupling; Motion; Aerospace engineering.

Author keywords: Multiple gyroscopes; Fundamental equation; Synchronization; Constrained motion; Nonlinear control; Chain-coupled; General-coupled.

Introduction

Gyroscopes have long been used in navigation to measure orientation. From aerospace vehicles to consumer electronic devices, gyroscopes have played an important role in our everyday lives. From an engineering point of view, gyroscopes are highly nonlinear mechanical systems that exhibit a plethora of complicated motions such as periodic behavior, period-doubling behavior, quasi-periodic behavior, and chaotic behavior. Studies (Tong and Mrad 2001; Ge and Chen 1996; Ge et al. 1996; Van Dooren 2003) have shown that when a symmetric gyroscope with linear plus cubic damping is subjected to a harmonic vertical base excitation, the motion thus obtained can range from regular motion to chaotic motion depending on the parameters selected.

In analytical mechanics, the problem of synchronization of multiple chaotic systems has been of particular interest in recent times (Leipnik and Newton 1981; Pecora and Carroll 1990). In particular, the problem of synchronizing a set of slave gyroscopes, which may or may not be coupled to each other, to an independent master gyroscope is an important problem in nonlinear dynamics that has received considerable attention (Chen 2002; Lei et al. 2005; Udwadia 2008). This problem gains prominence in the field of spacecraft dynamics where attitude control of spacecraft is almost always performed using gyroscopes. When there are multiple gyroscopes onboard a spacecraft, it is often required that they be synchronized to indicate a specific, usable spacecraft pointing. And

given that these gyroscopes exhibit a wide range of dynamic behavior, the problem of synchronization becomes even more challenging. The synchronization problem also finds applications in areas of secure communication (e.g., transmission of encrypted messages) and in areas of signal processing (Strogatz 2000). A large number of papers written on this subject only seem to consider the synchronization problem of two identical gyroscopes. Chen (2002) considers two identical chaotic gyros with different initial conditions and uses numerous classical control laws to show that when the feedback gain (obtained through experimentation) exceeds a particular value, the slave gyro synchronizes with the master gyro. Lei et al. (2005) approach the same problem using feedback linearization wherein the difference in response between the master and slave gyro is taken as an error signal and a time-varying control is chosen to drive the error signal to zero. Aghababa (2011), on the other hand, considers an adaptive robust finite-time controller to synchronize two chaotic gyros despite unknown uncertainties in the system. These approaches to the synchronization of master/slave gyros appear to work when the number of slaves considered is small in number. However, when a large number of slaves with nonidentical physical and geometric properties are considered, the need to develop efficient control methods arise. It is also important to note that many papers on this subject assume that the gyroscopes are in the so-called sleeping position, which in general is an oversimplifying condition, because most gyroscopes do not satisfy it.

Recently, Udwadia and Han (2008) approached the problem of synchronization of multiple chaotic gyroscopes from a new perspective—using the constrained motion approach. In their paper, Udwadia and Han consider a system of n gyroscopes, each in the so-called sleeping position, which are all uncoupled from one another, and have varying physical and geometrical properties, some or all of which exhibit chaotic behavior. They attempt to synchronize these uncoupled slave gyros with a master gyro. The problem of synchronization, which is classically considered as a tracking control problem in control theory, is recast as a problem of constrained

¹Ph.D. Candidate, Dept. of Aerospace and Mechanical Engineering, Univ. of Southern California, Los Angeles, CA 90089. E-mail: mylapill@usc.edu

Note. This manuscript was submitted on August 16, 2011; approved on December 14, 2011; published online on December 16, 2011. Discussion period open until March 1, 2014; separate discussions must be submitted for individual papers. This paper is part of the *Journal of Aerospace Engineering*, Vol. 26, No. 4, October 1, 2013. ©ASCE, ISSN 0893-1321/2013/4-814-828/\$25.00.

motion. The slaves are suitably constrained and the fundamental equation (Udwadia and Kalaba 1996a) is used in arriving at the nonlinear control torques that force exact synchronization of each slave gyro with the master gyro. However, the problem with synchronizing a master gyro with n uncoupled slave gyroscopes is that it can effectively be simplified into n separate problems of synchronization of the master gyro with n individual slave gyros.

In this paper, we consider a set of n coupled gyros such that they form a single system of interacting slave gyroscopes. Next, we attempt to synchronize this nonlinear system of slave gyros with an independent master gyroscope whose motion can be either regular or chaotic. We adopt the methods developed by Udwadia and Han (2008) and build on them to derive the constrained equations of motion for the case when the slave gyroscopes are all coupled. In the process, we also obtain explicit and closed-form expressions for the generalized nonlinear control torques that are required to be applied to each of the slave gyros to obtain synchronization with the master gyro. We consider both linear and highly nonlinear types of coupling [which include linear plus cubic coupling, sinusoidal coupling, and Toda coupling (Toda 1981)] between the slave gyroscopes. The effect of the sleeping condition on the synchronization of the gyros is also studied. Further, utilizing the concept of an incidence matrix, we also examine the case when the slave gyroscopes are coupled in a more general fashion (instead of the usual chain coupling). Finally, to illustrate the efficacy of the methods presented in this paper, we provide three numerical simulations. We consider a system of five gyros with one master and four chain-coupled slaves where the slaves are coupled (1) using sinusoidal coupling and then (2) using Toda coupling. In the Toda coupling case, the effect of the no-sleeping condition on the synchronization of the gyros is studied. The third example consists of a system of six gyroscopes with one master and five slaves where the slaves are coupled to one another through an incidence matrix with different types of strongly nonlinear couplings.

Equations of Motion

Consider the system of $n + 1$ symmetric gyroscopes as shown in Figs. 1 and 2. The master gyro whose parameters are denoted by the subscript m is an independent system separate from the slave

gyroscopes. The other n gyroscopes (denoted by subscripts $1 - n$) are all coupled together with torsion springs to form the system of slave gyros. In the current study, we use Euler angles to describe the orientation of each gyroscope— θ (nutation), φ (precession), and ψ (spin).

Master Gyroscope

The nonlinear equation of motion of a symmetric gyroscope whose point of support O is subjected to a vertical harmonic excitation of frequency ω_m and amplitude \tilde{d}_m has been derived by Udwadia and Han (2008) and is reproduced as

$$I_m \ddot{\theta}_m + \frac{(p_{\varphi_m} - p_{\psi_m} \cos \theta_m)(p_{\psi_m} - p_{\varphi_m} \cos \theta_m)}{I_m \sin^3 \theta_m} - m_m g r_m \sin \theta_m \\ - m_m r_m \sin \theta_m \ddot{d}_m(t) = F_d \quad (1)$$

where the angular momenta $p_{\psi_m} = I_{3_m}(\dot{\psi}_m + \dot{\varphi}_m \cos \theta_m)$ and $p_{\varphi_m} = I_m \dot{\varphi}_m \sin^2 \theta_m + p_{\psi_m} \cos \theta_m$ are conserved quantities as ψ_m , φ_m are cyclic coordinates; m_m = mass of the master gyroscope, $I_m = I_{1_m} + m_m r_m^2$, where $I_{1_m} = I_{2_m}$ = principal equatorial moment of inertia of the master gyroscope and I_{3_m} = polar moment of inertia; θ_m , ψ_m , φ_m = Euler angles of rotation associated with the master gyroscope; r_m = distance along the polar axis of the center of mass of the gyro from its point of support (see Fig. 1); and $d_m(t) = d_m \sin(\omega_m t)$ = time-varying amplitude of the vertical support motion that has frequency ω_m . The nonconservative damping force acting on the master gyroscope $F_d = -\tilde{c}_m \dot{\theta}_m - \tilde{e}_m \dot{\theta}_m^3$ is assumed to be of linear plus cubic type (Ge et al. 1996). A stationary symmetric gyro positioned with its axis along the vertical usually falls over. However, when it is given a sufficiently large spin about the vertical axis, it begins to rotate in a stable fashion, with its axis remaining very close to the vertical. The symmetric gyro showing this type of sleeping-top motion is said to be in a sleeping position and this usually happens when the angular momenta ($p_\psi = p_\varphi = p$) is constant for all time t . The equation of motion of the vertically excited master gyro [Eq. (1)] in the sleeping position is then given by

$$\underbrace{\ddot{\theta}_m + \alpha_m^2 \frac{(1 - \cos \theta_m)^2}{\sin^3 \theta_m} + c_m \dot{\theta}_m + e_m \dot{\theta}_m^3 - \beta_m \sin \theta_m + \gamma_m \sin \theta_m \sin(\omega_m t)}_{-F_m^{\text{gyro}}} = 0 \quad (2)$$

where

$$P_m = \left\{ \begin{array}{l} \alpha_m = \frac{p_m}{I_m}, \beta_m = \frac{m_m g r_m}{I_m}, c_m = \frac{\tilde{c}_m}{I_m}, e_m = \frac{\tilde{e}_m}{I_m}, \\ \gamma_m = \frac{m_m r_m \tilde{d}_m \omega_m^2}{I_m}, \omega_m, I_m \end{array} \right\}$$

is the parameter set that describes the physical characteristics of the master gyroscope.

Slave Gyroscopes

Consider the system of n symmetric gyroscopes that are coupled in chain fashion as shown in Fig. 2. The subscript i (where $i = 1 - n$) denotes each individual slave gyro. Each of the slave gyros is subjected to a vertical harmonic base excitation of amplitude \tilde{d}_i and frequency ω_i . The slaves are also subjected to a nonconservative damping force that is of linear plus cubic type related only to the θ -coordinate. The following types of torsion spring couplings are studied in the present paper:

1. Harmonic coupling

$$V_i^t(\theta_{i+1} - \theta_i) = \sigma_i [1 - \cos(\theta_{i+1} - \theta_i)] \quad (3)$$

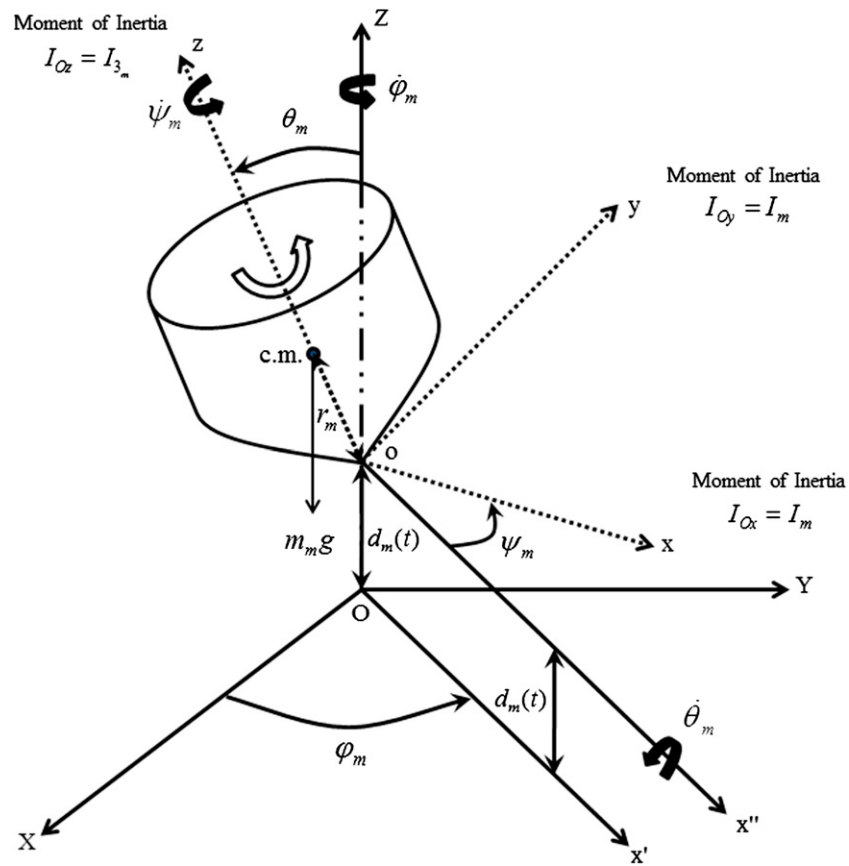


Fig. 1. Symmetrical master gyro (independent) subjected to a vertical harmonic excitation

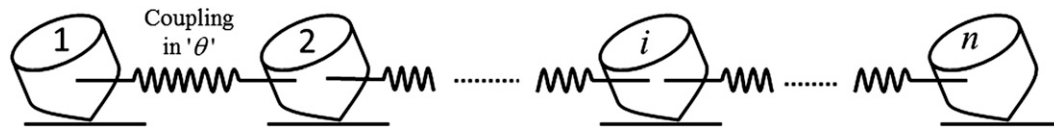


Fig. 2. A system of chain-coupled slave gyroscopes; each slave gyro in the chain is subjected to a vertical harmonic excitation which, when uncoupled from the system, results in regular or chaotic motion

2. Toda torsion coupling (Toda 1981)

$$V_i^t(\theta_{i+1} - \theta_i) = \frac{a_i}{b_i} e^{b_i(\theta_{i+1} - \theta_i)} - a_i(\theta_{i+1} - \theta_i) - \frac{a_i}{b_i} \quad (4)$$

3. Linear plus cubic coupling

$$V_i^t(\theta_{i+1} - \theta_i) = \frac{f_i}{2} (\theta_{i+1} - \theta_i)^2 + \frac{g_i}{4} (\theta_{i+1} - \theta_i)^4 \quad (5)$$

where a_i , b_i , f_i , g_i , and σ_i = spring constants corresponding to the i th spring element and V_i^t = torsional potential energy of the i th spring element in the chain.

Consider the i th gyroscope in the slave system. Besides the forces F_i^{gyro} [see Eq. (6)] that act on a symmetric gyro as a consequence of it being subjected to nonlinear damping and vertical excitation, the only additional forces that act on it are the coupling forces. Thus, the equation of motion of the i th slave gyroscope in the θ_i direction can be computed using Newton's laws as follows:

$$\ddot{\theta}_i + \underbrace{\left(\frac{(p_{\varphi_i} - p_{\psi_i} \cos \theta_i)(p_{\psi_i} - p_{\varphi_i} \cos \theta_i)}{I_i^2 \sin^3 \theta_i} + \frac{\tilde{c}_i}{I_i} \dot{\theta}_i + \frac{\tilde{e}_i}{I_i} \dot{\theta}_i^3 - \frac{m_i g r_i}{I_i} \sin \theta_i - \frac{m_i r_i}{I_i} \sin \theta_i \ddot{d}_i(t) \right)}_{-F_i^{\text{gyro}}} = \underbrace{\frac{1}{I_i} \left[\frac{\partial V^t(\theta_{i+1} - \theta_i)}{\partial \theta_i} - \frac{\partial V^t(\theta_i - \theta_{i-1})}{\partial \theta_i} \right]}_{F_{i+1,i}^S - F_{i,i-1}^S} \quad (6)$$

where $p_{\psi_i} = I_3(\dot{\psi}_i + \dot{\varphi}_i \cos \theta_i)$, $p_{\varphi_i} = I_1 \dot{\varphi}_i \sin^2 \theta_i + p_{\psi_i} \cos \theta_i$, $d_i(t) = \tilde{d}_i \sin(\omega_i t)$, and $F_{i+1,i}^{\text{sin}} = \sigma_i \sin(\theta_{i+1} - \theta_i)$ for a harmonic coupling; $F_{i+1,i}^{\text{Toda}} = a_i [e^{b_i(\theta_{i+1} - \theta_i)} - 1]$ for a Toda coupling; and $F_{i+1,i}^{\text{LC}} = f_i(\theta_{i+1} - \theta_i) + g_i(\theta_{i+1} - \theta_i)^3$ for a linear plus cubic coupling. Because ψ_i and φ_i are cyclic coordinates, Eq. (6) alone is sufficient to describe the equation of motion of the i th slave gyro. Eq. (6) can be represented more conveniently as

$$\ddot{\theta}_i = F_i^{\text{gyro}} + \frac{1}{I_i} (F_{i+1,i}^S - F_{i,i-1}^S) \quad (7)$$

where F_i^{gyro} = gyroscopic forces acting on the i th gyro from its being subjected to vertical excitation and nonlinear damping and $F_{i+1,i}^S$ is the coupling force exerted by the $(i+1)$ th gyro on the i th gyro. In the current study, we approach the problem of synchronization of multiple gyroscopes from a constrained motion perspective, which includes three vital steps: (1) derivation of the equations of motion of the unconstrained system; (2) formulation of the constraint equations; and (3) use of the fundamental equation (Udwadia and Kalaba 1996a, b) to obtain the constrained equations of motion of synchronized master-slave system.

In the process, we also find a closed-form expression for the explicit nonlinear control torques that are required to be applied to each of the slave gyroscopes to synchronize them precisely with the motion of the master gyroscope.

Unconstrained Equations of Motion

In the present paper, the independent master gyroscope [Eq. (1)] along with the system of coupled slave gyroscopes [Eq. (7)] forms the unconstrained system (Udwadia and Kalaba 1996a, b). The unconstrained equation of motion of the system can be written in matrix form [using Eqs. (2) and (6)] as follows:

$$M_{(n+1) \times (n+1)} \underbrace{\begin{bmatrix} \ddot{\theta}_m \\ \ddot{\theta}_1 \\ \vdots \\ \ddot{\theta}_i \\ \vdots \\ \ddot{\theta}_n \end{bmatrix}}_{\ddot{\mathbf{X}}_{n+1 \times 1}} = \underbrace{\begin{bmatrix} F_m^{\text{gyro}} & F_m^{\text{gyro}} \\ F_1^{\text{gyro}} & + F_{2,1}^S / I_1 \\ \vdots & \vdots \\ F_i^{\text{gyro}} & + (F_{i+1,i}^S - F_{i,i-1}^S) / I_i \\ \vdots & \vdots \\ F_n^{\text{gyro}} & + (-F_{n,n-1}^S) / I_n \end{bmatrix}}_{F_{n+1 \times 1}} \quad (8)$$

where M = identity matrix of size $n+1$; and $a = M^{-1}F = F$ = unconstrained acceleration of the system. To this unconstrained system, we impose a set of constraints such that the system of coupled slave gyroscopes precisely follows the master gyroscope in its motion.

Constraint Equations

The unconstrained system from Eq. (8) is subjected to the following set of constraints:

No Control Force on the Master Gyro

Because the motion of the master gyroscope is considered to be independent of the motion of the slave gyroscopes, the need to apply a control force on the master gyro does not arise in the

constrained system. Hence, the unconstrained motion of the master gyroscope can itself be considered as a constraint equation. Thus, we have

$$\ddot{\theta}_m = F_m^{\text{gyro}} \quad (9)$$

Synchronization Constraint

In the present paper, our goal is to synchronize the motion of each of the coupled slave gyroes with that of the master gyro. Hence, the following set of n constraints are imposed on the unconstrained system and are given by

$$v_i = \theta_m - \theta_i = 0, \quad i = 1, 2, 3, \dots, n \quad (10)$$

The initial conditions of these slave gyroes are assumed to satisfy the constraint equations. However, it may not always be possible to initiate the slave gyroes from positions in phase space that satisfy the constraints. This problem is surmounted by choosing appropriate trajectory stabilization parameters δ, k (Udwadia 2003, 2008) such that

$$\ddot{v}_i + \delta \dot{v}_i + k v_i = 0 \Rightarrow \ddot{\theta}_m - \ddot{\theta}_i = -\delta (\dot{\theta}_m - \dot{\theta}_i) - k(\theta_m - \theta_i) \quad (11)$$

Thus, the unconstrained system in Eq. (8) is subjected to a total of $n+1$ cumulative constraints to achieve synchronization of each individual coupled slave gyro with the motion of the master gyro. When the constraints in Eqs. (9) and (11) are expressed in the constraint matrix form, we obtain

$$\underbrace{\begin{bmatrix} [1] & [0 & \cdots & 0] \\ [1] & [-I_n \text{ by } n] \\ \vdots & \vdots \\ [1] & \end{bmatrix}}_{A_{n+1 \times n+1}} \underbrace{\begin{bmatrix} \ddot{\theta}_m \\ \ddot{\theta}_1 \\ \vdots \\ \ddot{\theta}_i \\ \vdots \\ \ddot{\theta}_n \end{bmatrix}}_{\ddot{\mathbf{X}}_{n+1 \times 1}} = \underbrace{\begin{bmatrix} F_m^{\text{gyro}} \\ -\delta (\dot{\theta}_m - \dot{\theta}_1) - k(\theta_m - \theta_1) \\ \vdots \\ -\delta (\dot{\theta}_m - \dot{\theta}_i) - k(\theta_m - \theta_i) \\ \vdots \\ -\delta (\dot{\theta}_m - \dot{\theta}_n) - k(\theta_m - \theta_n) \end{bmatrix}}_{b_{n+1 \times 1}} \quad (12)$$

Constrained Equations of Motion

With all the requisite matrices (M, F, A, b) at our disposal, the constrained equations of motion can now be calculated using the fundamental equation (Udwadia and Kalaba 2002). Because $M = I_{n+1}$ and A = square matrix of size $n+1$, the expression for the control force reduces to

$$\begin{aligned} F^C &= M^{1/2} (AM^{-1})^+ (b - Aa) = A^+ (b - Aa) \\ &= A^{-1} (b - Aa) \end{aligned} \quad (13)$$

The constraint matrix A is structured in such a way that it possesses the unique property $A^{-1} = A$, and this reduces the explicit expression of the nonlinear control torques to

$$F^C = A^{-1}(b - Aa) = A^{-1}b - A^{-1}Aa = Ab - a$$

$$\begin{aligned}
&= \begin{bmatrix} [1] & [0 \ \cdots \ 0] \\ \begin{bmatrix} 1 \\ \vdots \\ 1 \end{bmatrix} & [-I_{n \times n}] \end{bmatrix} \begin{bmatrix} F_m^{\text{gyro}} \\ -\delta(\dot{\theta}_m - \dot{\theta}_1) - k(\theta_m - \theta_1) \\ \vdots \\ -\delta(\dot{\theta}_m - \dot{\theta}_i) - k(\theta_m - \theta_i) \\ \vdots \\ -\delta(\dot{\theta}_m - \dot{\theta}_n) - k(\theta_m - \theta_n) \end{bmatrix} - \begin{bmatrix} F_m^{\text{gyro}} \\ F_1^{\text{gyro}} + F_{2,1}^S/I_1 \\ \vdots \\ F_i^{\text{gyro}} + (F_{i+1,i}^S - F_{i,i-1}^S)/I_i \\ \vdots \\ F_n^{\text{gyro}} + (-F_{n,n-1}^S)/I_n \end{bmatrix} \\
&= \left\{ \begin{array}{c} 0 \\ \left[\delta(\dot{\theta}_m - \dot{\theta}_1) + k(\theta_m - \theta_1) \right] + F_m^{\text{gyro}} - \left(F_1^{\text{gyro}} + \frac{F_{2,1}^S}{I_1} \right) \\ \vdots \\ \left[\delta(\dot{\theta}_m - \dot{\theta}_i) + k(\theta_m - \theta_i) \right] + F_m^{\text{gyro}} - \left(F_i^{\text{gyro}} + \frac{F_{i+1,i}^S - F_{i,i-1}^S}{I_i} \right) \\ \vdots \\ \left[\delta(\dot{\theta}_m - \dot{\theta}_n) + k(\theta_m - \theta_n) \right] + F_m^{\text{gyro}} - \left(F_n^{\text{gyro}} + \frac{-F_{n,n-1}^S}{I_n} \right) \end{array} \right\} \quad (14)
\end{aligned}$$

where δ and k = trajectory stabilization parameters and F^{gyro} and F^S = gyroscopic forces and coupling forces, respectively. Thus, Eq. (14) gives us the explicit, closed-form expression for the nonlinear control torques (devoid of any approximations or simplifications) that need to be applied to the unconstrained system to obtain the constrained system. The constrained equations of motion of the system (Udwadia and Kalaba 1996a, b, 2002) can now be written as

$$M\ddot{X} = F + F^C \quad (15)$$

where F is given by the right-hand side of Eq. (8) and F^C is given by the Eq. (14). Eq. (15) represents the governing equations of motion of the coupled slave gyroscopes that follow a given independent master gyroscope, irrespective of its chaotic or regular motion.

Incidence Matrix

Until now, we have considered the case wherein the slave gyro are all coupled in a chain fashion. But it is indeed possible to consider a more general interaction of the slave gyroes wherein a particular slave gyro can be coupled to any number of other slave gyroes without any restrictions. Now, in such a case, it becomes imperative to keep track of the coupling information between any two slave gyroes in the system. This can be succinctly done by the use of an incidence matrix. The incidence matrix has the following salient features:

- The incidence matrix, denoted by ξ , is a symmetric matrix of size n (where n denotes the number of slave gyroes). It gives us information about the coupling between any two slave gyroes in the system.
- Each element of the incidence matrix ξ is restricted to have a value of either 0 or 1. A zero value of ξ_{ij} indicates that the i th

and j th slaves are uncoupled whereas a unitary value of ξ_{ij} indicates that the i th slave is coupled to the j th slave.

- Because a gyroscope cannot be coupled to itself, the diagonal elements of the incidence matrix are all zero (i.e., $\xi_{ii} = 0$; $i = 1, 2, 3, \dots, n$).

Thus, given an incidence matrix that describes the various different interactions between a set of coupled slave gyroes, the unconstrained equations of motion of the i th slave gyro in the system can be written as follows:

$$\ddot{\theta}_i = F_i^{\text{gyro}} + \frac{1}{I_i} \left(\sum_{\substack{j=1 \\ j \neq i}}^n \xi_{ij} F_{ij}^{\text{Couple}} \right), \quad i = 1, 2, 3, \dots, n \quad (16)$$

where $F_{ij}^{\text{Couple}} = -F_{ji}^{\text{Couple}}$. This set of n equations along with the unconstrained motion of the independent master gyro [Eq. (2)] forms the unconstrained system. The reader can now utilize the methods described in this section to rederive the constrained equations of motion of the master-slave system and generate the necessary control torques that are required to be applied to the slave system of gyroscopes such that they synchronize precisely with the motion of the master gyroscope.

Results and Simulations

To better illustrate the efficacy of the methods presented in this paper, we present three numerical simulations. In the first example, we consider a system of five gyroes (1 Master + 4 Slaves) with the sleeping condition imposed on all five gyroes. We examine the effect of

sinusoidally chain coupling the slave gyros on the synchronization of the gyros. In the second example, we consider a system of six gyros (1 Master + 5 Slaves) and use an incidence matrix to describe the various different interactions between the five coupled slave gyros. The sleeping condition is imposed on all six gyros and different types of linear and nonlinear couplings are used to couple the individual slaves. In the third example, we consider a five-gyro system (1 Master + 4 Slaves) and explore the effect of the sleeping condition on the synchronization of the gyros.

Throughout this paper, the integration of the equations of motion (constrained as well as unconstrained) is performed using the ODE45 solver from the software *MATLAB* with a relative error tolerance of 10^{-9} and an absolute error tolerance of 10^{-12} . Further, the Lyapunov exponents for the master-slave system of gyros are computed using the methods described in Udwadia and von Bremen (2000, 2001, 2002) over a time span of 1,000 s. To determine these exponents, integration has been performed, once again, using the *MATLAB* ODE45 solver with a relative error tolerance of 10^{-9} and an absolute error tolerance of 10^{-13} .

Synchronization with the Use of a Sleeping Condition

Five Gyroscopes (1 Master + 4 Coupled Slaves) Using a Sine Coupling

Consider a system of five nonidentical gyroscopes (1 Master + 4 Slaves) where the set of four slave gyroscopes are all connected

in a chain fashion using a sinusoidal coupling [described by Eq. (3)] with coefficients $\sigma_{12} = 2$, $\sigma_{23} = 1.5$, and $\sigma_{34} = 2.5$. All gyros are assumed to be in the sleeping position and we have

$$p_{\varphi_i} = p_{\psi_i} = p_i, \quad i = m, 1, 2, 3, 4$$

Each individual slave gyro (although coupled to other slaves) is required to precisely track the motion of the master gyro. Table 1 gives the parameter sets

$$P_i = \{\alpha_i, \beta_i, c_i, e_i, \gamma_i, \omega_i, I_i\}, \quad i = m, 1, 2, 3, 4$$

that describe the characteristics of each of the gyros of the master-slave system and their initial condition sets

$$\text{IC}_i = [\theta_i^0, \dot{\theta}_i^0, \tau_i^0]$$

Using the parameters in Table 1, the Lyapunov exponents for the master gyroscope and the system of slave gyroscopes are computed, respectively, to be

$$l_m = \{-0.179707, -0.500232, 0\}$$

$$l_s = \left\{ \begin{array}{lll} 0.121455, & 0.066865, & 0.004824, \\ -0.568669, & -0.645423, & 0.000110, \\ -0.039699, & -0.253232, & 0.000107, \\ -0.728986, & -0.777867, & 0 \end{array} \right\}$$

Because the values of l_m are either negative or zero, the master gyro is said to exhibit regular periodic motion. The slave system, on the other hand, appears to be chaotic.

The unconstrained system consists of the master gyroscope and the set of four coupled slave gyroscopes whose equations of motion can be written using Eq. (8). Fig. 3 shows a phase plot $(\theta_m, \dot{\theta}_m)$ of the unconstrained motion of the master gyroscope. Clearly, the motion of the master is periodic, as also indicated by its Lyapunov exponents. Fig. 4, on the other hand, shows a phase plot $(\theta_i, \dot{\theta}_i)$, $i = 1, 2, 3, 4$ of the unconstrained motion of the individual slave gyroscopes. The phase plots (Figs. 3 and 4) are all plotted in the time range $150 \leq t \leq 200$ s. A superimposed image of the time history of the nutation angle θ of the five gyros is plotted in Fig. 5 showing that prior to synchronization, the five gyros exhibit highly nonlinear behavior and their trajectories vary widely from each other.

To this unconstrained system, we impose a set of five constraints [as described by Eq. (12) with trajectory stabilization constants $\delta = 1$ and $k = 2$] and compute the constrained equations of motion using Eq. (15). A superimposed phase plot of the constrained motion of the master-slave system of gyros is plotted in Fig. 6 for $150 \leq t \leq 200$. As can be seen from the figure, the four slave gyros which are all sinusoidally (chain) coupled to each other synchronize precisely with the periodic motion of the master gyroscope. Fig. 7 shows the time history of nutation angle θ post-synchronization; the control forces take less than 10 s to exponentially reduce the error between the motion of master and the individual slaves to zero. Fig. 8 shows a time history of synchronization errors for $60 \leq t \leq 200$. Note that the error converges exponentially as demanded by Eq. (11). The synchronization errors are approximately 10^{-13} , which is lower than the tolerance levels used in the *MATLAB* ODE45 solver showing

Table 1. Parameter and Initial Conditions Sets for the Five Gyroscopes

| Name | Parameter sets | Initial conditions |
|-----------------------------|---|-------------------------------|
| Master gyroscope (periodic) | $P_m = \{10.5, 1, 0.5, 0.02, 38.7, 2.2, 1\}$ | $\text{IC}_m = [-1, 0.5, 0]$ |
| 1st slave gyroscope | $P_1 = \{10.1, 0.5, 0.05, 35.5, 2, 1\}$ | $\text{IC}_1 = [0.5, 1, 0]$ |
| 2nd slave gyroscope | $P_2 = \{10.5, 1, 0.5, 0.04, 38.5, 2.1, 2\}$ | $\text{IC}_2 = [1, -0.5, 0]$ |
| 3rd slave gyroscope | $P_3 = \{10, 1, 0.5, 0.03, 35.8, 2.05, 1.5\}$ | $\text{IC}_3 = [-0.5, 1, 0]$ |
| 4th slave gyroscope | $P_4 = \{10.5, 1, 0.45, 0.045, 36, 2.05, 1.7\}$ | $\text{IC}_4 = [0.5, 0.5, 0]$ |

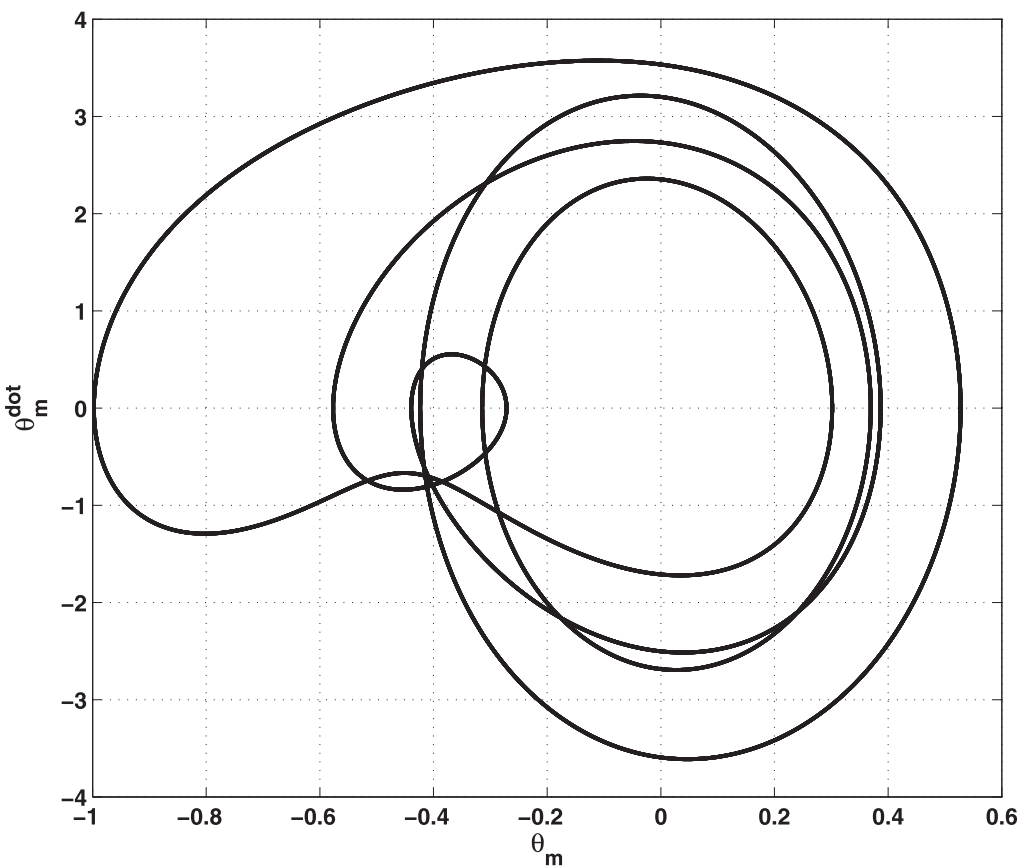


Fig. 3. A phase plot of the unconstrained motion of the periodic master gyroscope for $150 \leq t \leq 200$

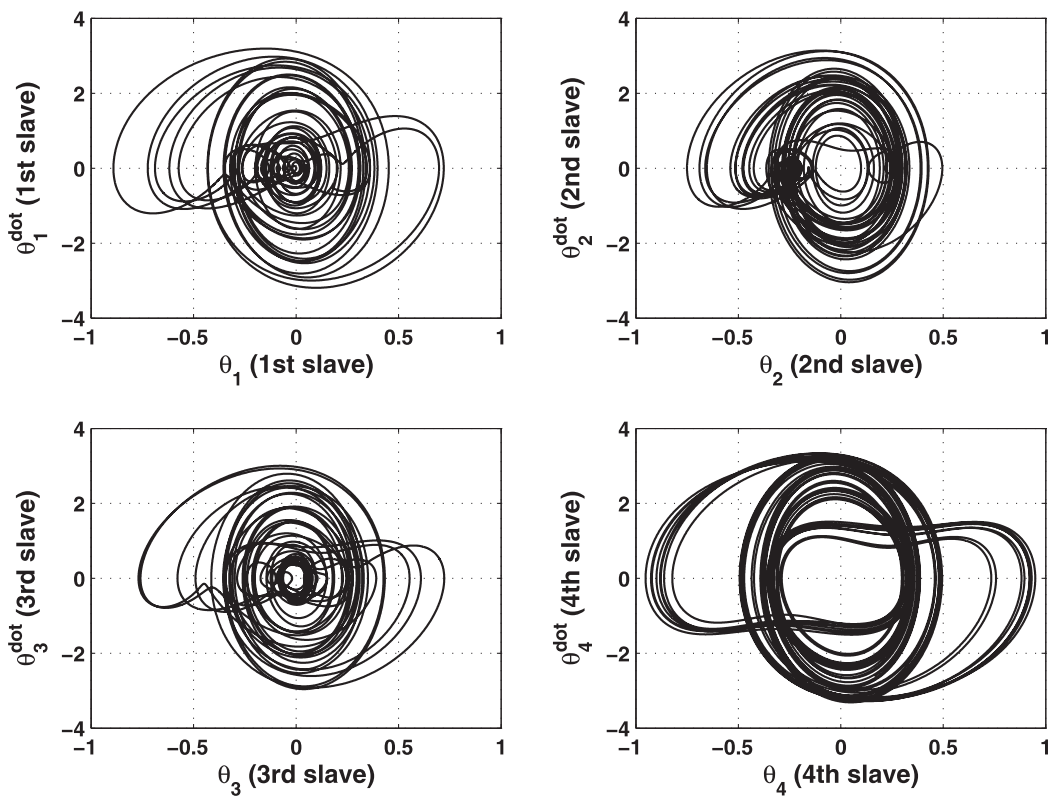


Fig. 4. A phase plot of the unconstrained motion of the four slave gyroscopes which are all coupled to one another in a chain fashion ($150 \leq t \leq 200$)

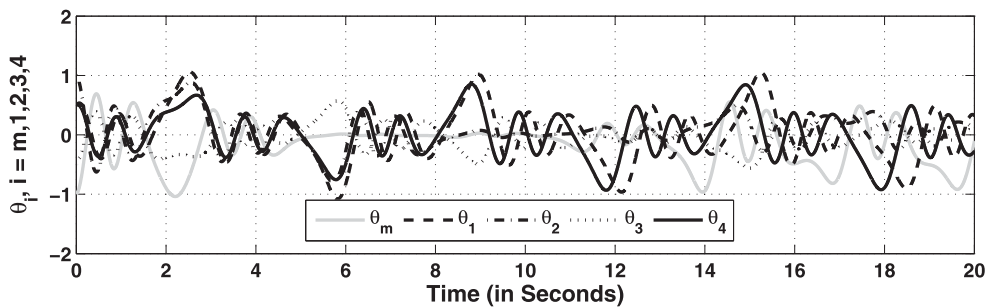


Fig. 5. Time history of θ for each individual gyroscope for $0 \leq t \leq 20$ prior to synchronization

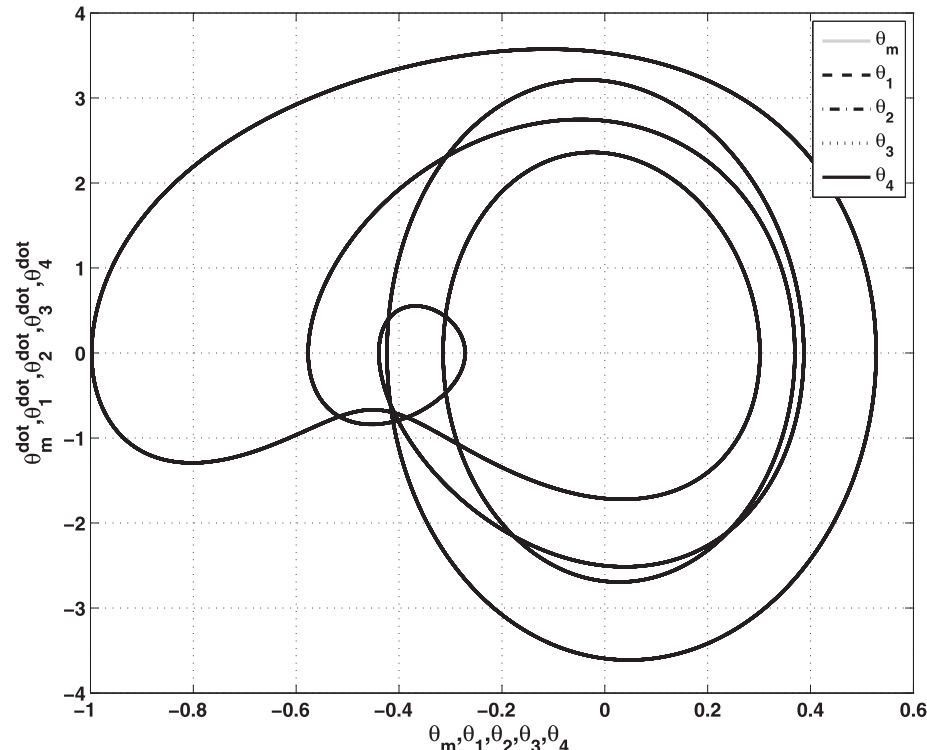


Fig. 6. A superimposed phase plot of the constrained motion of the five gyroscopes for $150 \leq t \leq 200$; the slave gyroscopes have precisely synchronized with the motion of the master gyro

the efficacy of the control forces in achieving synchronization. Thus, a system of four nonidentical slave gyros which are sinusoidally chain-coupled to each other have been shown to precisely track the motion of a master gyroscope exhibiting periodic motion.

Six Gyroscopes (1 Master + 5 Coupled Slaves) Using the Incidence Matrix

In the present example, we consider a system of six nonidentical gyroscopes (1 Master + 5 Coupled Slaves) where the interaction between the five slaves is more general and is described by an incidence matrix. The five coupled gyros are required to precisely track the motion of the independent master gyro [described by the parameter set P_m (see Table 2)], which in this case exhibits chaotic motion as seen from its Lyapunov exponents

$$l_m = \{ 0.206668, -0.896620, 0 \}$$

The coupling between the slaves (with parameter sets P_i , $i = 1, 2, 3, 4, 5$ given in Table 2) is described by the 5×5 incidence matrix ξ , shown as

$$\xi = \begin{bmatrix} 0 & 1_T & 0 & 1_L & 1_S \\ 1_T & 0 & 1_S & 0 & 1_L \\ 0 & 1_S & 0 & 1_{LC} & 0 \\ 1_L & 0 & 1_{LC} & 0 & 0 \\ 1_S & 1_L & 0 & 0 & 0 \end{bmatrix} \quad (17)$$

The interaction between the i th and j th slaves is characterized by the value of the (i, j) th element of the matrix ξ . The subscripts L , S , T , and LC of the (i, j) th element of the incidence matrix denotes Linear, Sinusoidal, Toda, and Linear + Cubic couplings, respectively. Fig. 9 is a pictorial representation of the incidence matrix showing the various types of couplings applied between the individual slave

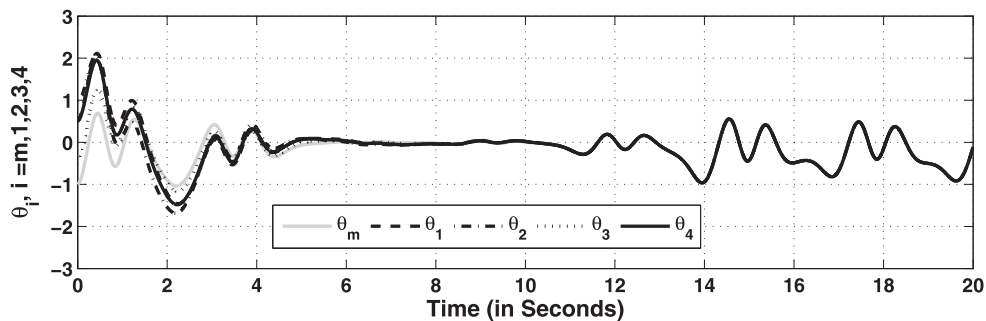


Fig. 7. Time history of θ for each individual gyroscope for $0 \leq t \leq 20$ in the constrained system; slave gyros take less than 10 s to synchronize with the motion of the master gyro

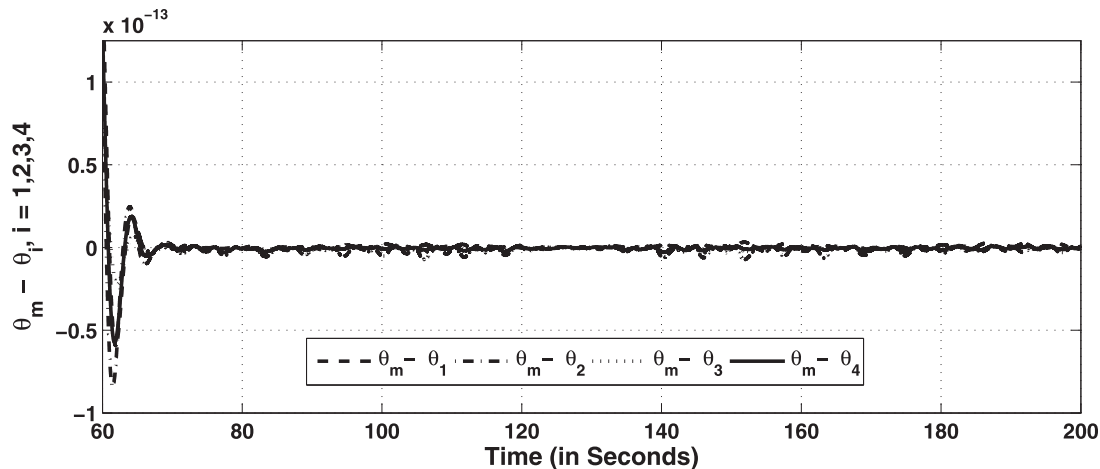


Fig. 8. Time history of synchronization errors for $60 \leq t \leq 200$; errors are smaller than the tolerance levels of the integration scheme

Table 2. Parameter and Initial Condition Sets for the Six Gyroscopes

| Name | Parameter sets | Initial conditions |
|----------------------------|---|------------------------|
| Master gyroscope (chaotic) | $P_m = \{10, 1, 0.5, 0.03, 35.8, 2.05, 1\}$ | $IC_m = [-0.5, 1, 0]$ |
| 1st slave gyroscope | $P_1 = \{10, 1, 0.5, 0.05, 35.5, 2, 2\}$ | $IC_1 = [0.5, 1, 0]$ |
| 2nd slave gyroscope | $P_2 = \{10.5, 1, 0.5, 0.04, 38.5, 2.1, 1.3\}$ | $IC_2 = [1, -0.5, 0]$ |
| 3rd slave gyroscope | $P_3 = \{10.5, 1, 0.5, 0.02, 38.7, 2.2, 0.9\}$ | $IC_3 = [-1, 0.5, 0]$ |
| 4th slave gyroscope | $P_4 = \{10.5, 1, 0.45, 0.045, 36, 2.05, 1.5\}$ | $IC_4 = [0.5, 0.5, 0]$ |
| 5th slave gyroscope | $P_5 = \{10.5, 1, 0.5, 0.05, 38.5, 2, 1.7\}$ | $IC_5 = [0.5, -1, 0]$ |

gyroscopes. The unconstrained equation of motion of the master [Eq. (2)] and the five coupled slave gyroscopes [Eq. (16)], which are all assumed to be in the sleeping position, can now be written as

$$\ddot{\theta}_m = F_m^{\text{gyro}} \quad (18)$$

$$\ddot{\theta}_1 = F_1^{\text{gyro}} + \frac{1}{I_1} (F_{12}^{\text{Toda}} + F_{14}^{\text{Linear}} + F_{15}^{\text{Sine}}) \quad (19)$$

$$\ddot{\theta}_2 = F_2^{\text{gyro}} + \frac{1}{I_1} (F_{21}^{\text{Toda}} + F_{23}^{\text{Sine}} + F_{25}^{\text{Linear}}) \quad (20)$$

$$\ddot{\theta}_3 = F_3^{\text{gyro}} + \frac{1}{I_1} (F_{32}^{\text{Sine}} + F_{34}^{\text{Linear+Cubic}}) \quad (21)$$

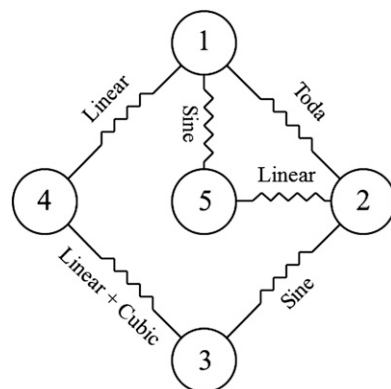


Fig. 9. General-coupled slave gyroscope system depicting various types of coupling/interactions between the slaves

$$\ddot{\theta}_4 = F_4^{\text{gyro}} + \frac{1}{I_1} (F_{41}^{\text{Linear}} + F_{43}^{\text{Linear+Cubic}}) \quad (22)$$

$$\ddot{\theta}_5 = F_5^{\text{gyro}} + \frac{1}{I_1} (F_{51}^{\text{Sine}} + F_{52}^{\text{Linear}}) \quad (23)$$

where F_i^{gyro} = definition given by Eq. (6); $F_{ij}^{\text{Toda}} = a_{ij}[e^{b_{ij}(\theta_j - \theta_i)} - 1]$; $F_{ij}^{\text{Sine}} = \sigma_{ij} \sin(\theta_j - \theta_i)$; $F_{ij}^{\text{Linear}} = \lambda_{ij} (\theta_j - \theta_i)$; $F_{ij}^{\text{Linear+Cubic}} = f_{ij}(\theta_j - \theta_i) + g_{ij}(\theta_j - \theta_i)^3$; and $F_{ij}^{\text{Couple}} = -F_{ij}^{\text{Couple}} \forall i < j$,

$i, j = 1, 2, 3, 4, 5$. The spring constants are given by the following parameters:

$$\begin{cases} a_{12} = 1.5, & b_{12} = 0.05, & \lambda_{14} = 0.5, & \sigma_{15} = 2, \\ \sigma_{23} = 1.2, & \lambda_{25} = 0.3, & f_{34} = 0.8, & g_{34} = 0.04 \end{cases}$$

From these parameters, the Lyapunov exponents for the system of slave gyros are calculated to be

$$l_s = \begin{cases} 0.082678, & 0.051033, & 0.015758, & -0.007526, & -0.075204, & 0.000197, & -0.424779, \\ -0.483015, & 0.000402, & -0.523197, & -0.646143, & 0.000002, & -0.723966, & -0.787581, & 0 \end{cases}$$

Based on these exponents, the slave system appears to be chaotic.

Fig. 10 shows phase plots $(\theta_i, \dot{\theta}_i)$, $i = m, 1, 2, 3, 4, 5$ of the unconstrained system from Eqs. (18)–(23) for $50 \leq t \leq 100$. The master gyroscope exhibits chaotic motion as predicted by l_m . From Fig. 10, we can infer that all six gyro exhibit highly nonlinear behavior and are unsynchronized. The constrained (synchronized) equations of motion for this system of six gyros can once again be computed using Eq. (15) with the application of six constraints [see Eq. (12)]. The phase plots of the constrained system $(\theta_i \text{ vs. } \dot{\theta}_i)$, $i = m, 1, 2, 3, 4, 5$ have been plotted in Fig. 11 for (a) $50 \leq t \leq 100$ and (b) $150 \leq t \leq 200$, where we observe that the plot of each gyro has been superimposed on top of another, indicating synchronization of the five slave gyros with the chaotic motion of the master. Fig. 12

shows a time history of the nutation angle θ for $0 \leq t \leq 20$. As can be inferred from the figure, it takes less than 10 s for the slave gyros to track the motion of the chaotic master gyro. Fig. 13 shows a time history of the synchronization errors in θ for each slave gyroscope in the time range of $60 \leq t \leq 200$. The vertical scale of the figure shows that the error is approximately 10^{-13} , signifying that the errors in the simulation are within the tolerance levels of the MATLAB ODE45 solver. A time history of the generalized control torques applied to each individual slave gyroscope to achieve synchronization with the chaotic master gyro is shown in Fig. 14. Thus, given a set of five nonidentical general-coupled slave gyros where the coupling between the gyros is prescribed by an incidence matrix, we managed to precisely synchronize the motion of the each of the slave gyros with

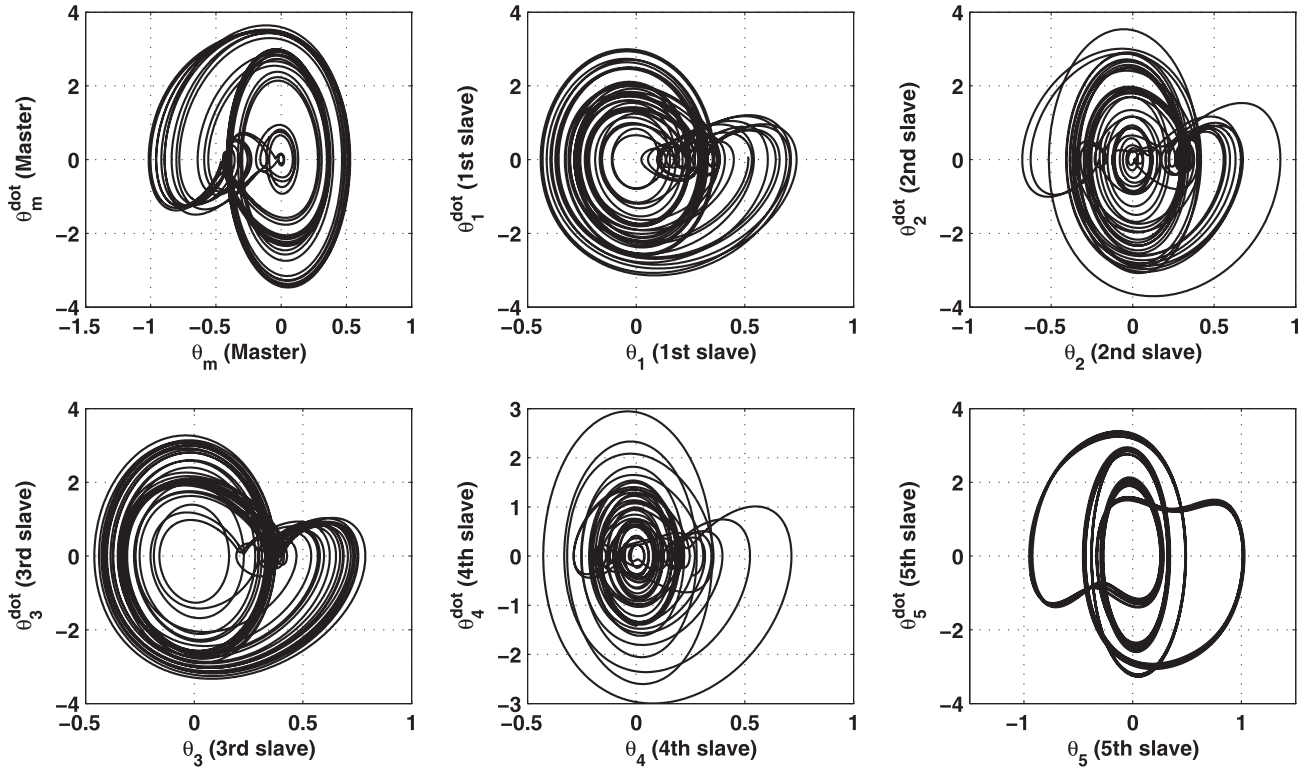


Fig. 10. Phase plots of the unconstrained motion for each individual gyroscope for $50 \leq t \leq 100$; the master gyroscope is independent whereas the other remaining five slave gyroscopes are all coupled using the incidence matrix

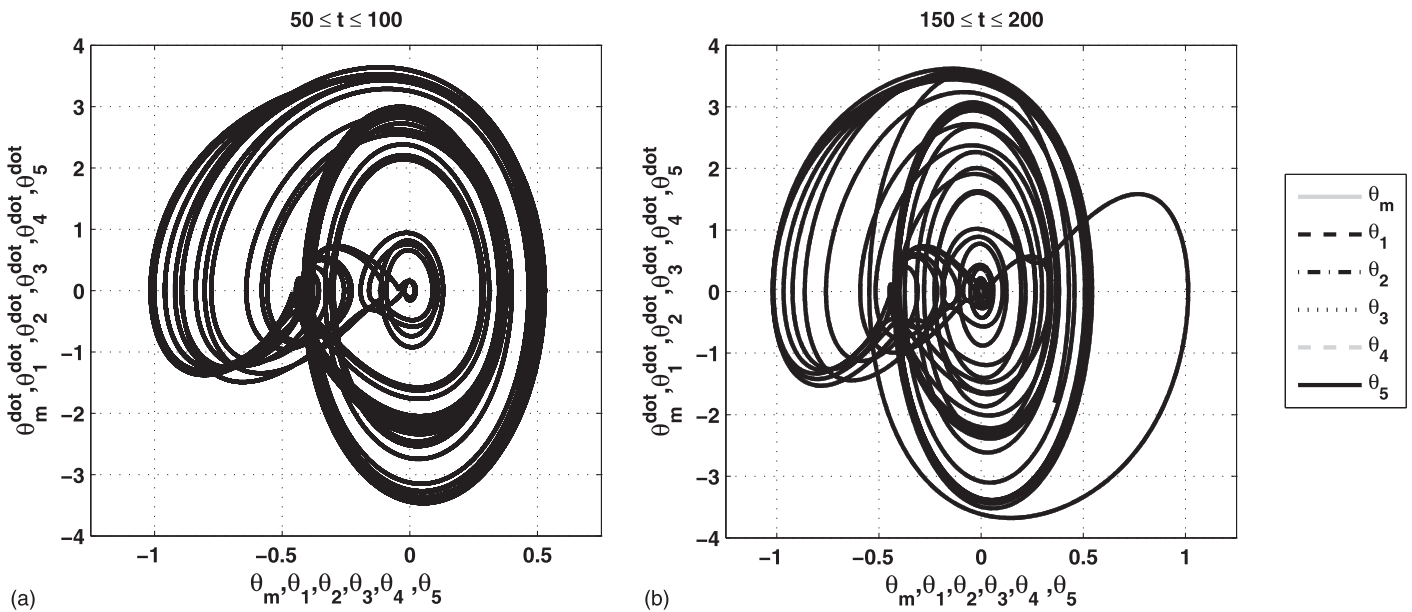


Fig. 11. Superimposed phase plots of the constrained motion of the five gyroscopes for (a) $50 \leq t \leq 100$ and (b) $150 \leq t \leq 200$; slave gyros have precisely tracked the motion of the master gyro

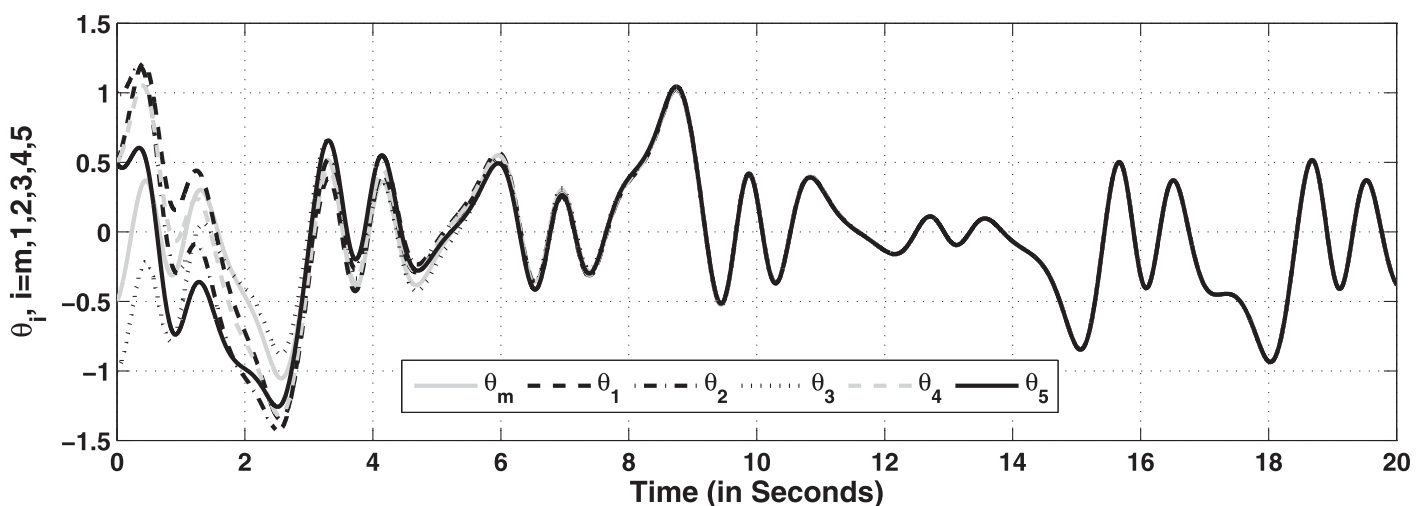


Fig. 12. Time history of θ for each individual gyroscope for $0 \leq t \leq 20$ in the constrained system

that of the chaotic master gyro, something quite significant for chaotic systems because they show extremely sensitive dependence to initial conditions.

Synchronization without the Use of the Sleeping Condition

In this section, we attempt to synchronize a set of nonidentical gyroscopes without using the so-called sleeping condition and show that synchronization can indeed be obtained even without the need to assume that the gyros are in sleeping position. If we remove the simplification of a sleeping condition, then we no longer assume that $p_{\varphi_i} = p_{\psi_i} = p_i$ and hence $p_{\varphi_i}, p_{\psi_i}$ can be chosen to be two different constants. Angular momenta $p_{\varphi_i}, p_{\psi_i}$ are associated with cyclic coordinates φ_i and ψ_i , respectively, and are therefore constant and cannot change with time. The imposition of the no-sleeping

condition brings an additional two parameters $p_{\varphi_i}, p_{\psi_i}$ into the dynamics of each individual gyroscope, and they are appended at the end of the set P to give the new parameter set

$$P_i = \left\{ \alpha_i = \frac{1}{I_i}, \beta_i = \frac{m_i g r_i}{I_i}, c_i = \frac{\tilde{c}_i}{I_i}, e_i = \frac{\tilde{e}_i}{I_i}, \gamma_i = \frac{m_i r_i \tilde{d}_i \omega_i^2}{I_i}, \omega_i, p_{\varphi_i}, p_{\psi_i} \right\}$$

Five Gyroscopes (1 Master + 4 Coupled Slaves) Using a Toda Coupling

Consider a system of five nonidentical gyroscopes (with parameter sets given by Table 3) where the set of four slave gyros are coupled in a chain fashion using a Toda torsion spring coupling. Each

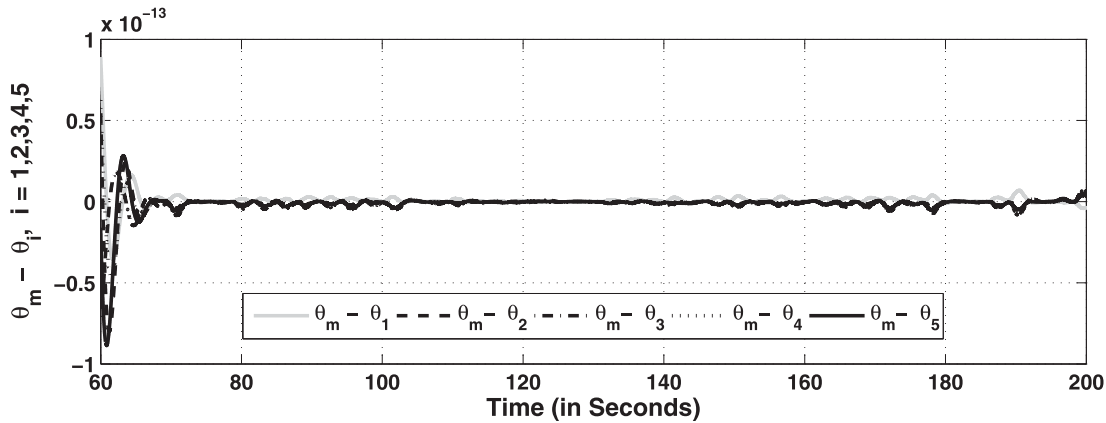


Fig. 13. Time history of synchronization errors for $60 \leq t \leq 200$; errors are smaller than the tolerance levels of the integration scheme

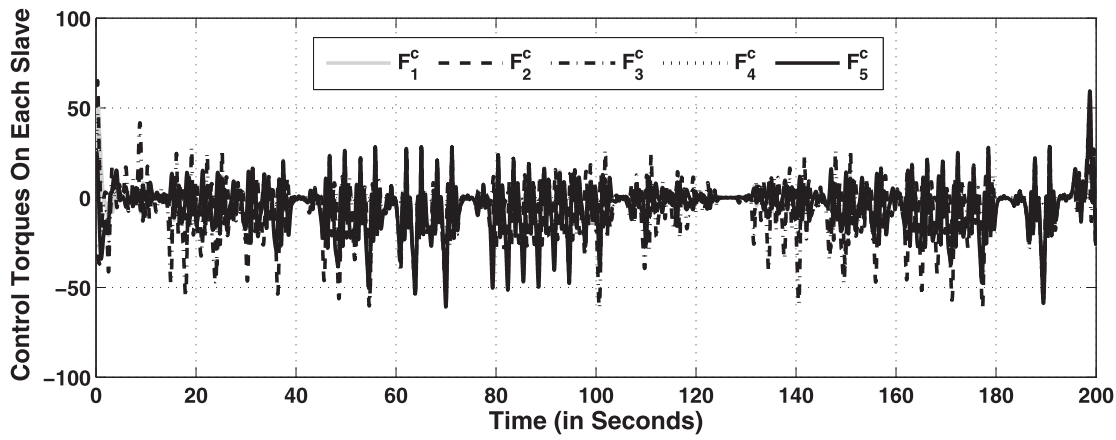


Fig. 14. Generalized control torques acting on each individual slave gyroscope for $0 \leq t \leq 200$

Table 3. Parameter and Initial Condition Sets for the Five Gyroscopes

| Name | Parameter sets | Initial conditions |
|-----------------------------|--|------------------------|
| Master gyroscope (periodic) | $P_m = \{2.5, 1.5, 0.45, 0.045, 35, 3, 1.5, 2.5\}$ | $IC_m = [1, -0.5, 0]$ |
| 1st slave gyroscope | $P_1 = \{1.35, 1.1, 0.44, 0.044, 36.1, 3, 1.9, 2.1\}$ | $IC_1 = [0.5, 1, 0]$ |
| 2nd slave gyroscope | $P_2 = \{1, 1.0, 0.44, 0.044, 35, 2.5, 2, 2.2\}$ | $IC_2 = [1, -0.5, 0]$ |
| 3rd slave gyroscope | $P_3 = \{1.04, 1.0, 0.45, 0.045, 36.0, 2.06, 1.5, 1.8\}$ | $IC_3 = [1, -1, 0]$ |
| 4th slave gyroscope | $P_4 = \{1, 1.1, 0.45, 0.045, 36.0, 2.05, 2.05, 2.15\}$ | $IC_4 = [0.5, 0.5, 0]$ |

individual coupled slave gyro is required to exactly track the motion of the master gyro

$$l_m = \{-0.223403, -0.226832, 0\}$$

which, in this case, exhibits regular periodic motion. The coefficients of the Toda spring elements are given by $a_{12} = 1.20$; $a_{23} = 1.50$; $a_{34} = 1.25$; $b_{12} = 0.11$; $b_{23} = 0.13$; and $b_{34} = 0.105$. The system of slave gyros appears to exhibit chaotic behavior, as indicated by its Lyapunov exponent set

$$l_s = \left\{ \begin{array}{ccccccc} 0.107805, & -0.015994, & 0.000394, & -0.121534, & -0.634956, & 0.000173, \\ -1.390733, & -1.850994, & 0.000002, & -1.881298, & -1.976043, & 0 \end{array} \right\}$$

Because the simplification of the sleeping condition is removed, the unconstrained equations of motion of the master and the individual slave gyros are given by Eqs. (1) and (6), respectively. A superimposed phase plot of the unconstrained motion of the periodic

master gyroscope ($\theta_m, \dot{\theta}_m$) along with the unconstrained motion of each individual coupled slave gyro ($\theta_i, \dot{\theta}_i$), $i = 1, 2, 3, 4$ is shown in Fig. 15. The phase plots are all plotted in the time range $50 \leq t \leq 100$. The nonidentical gyros exhibit highly nonlinear

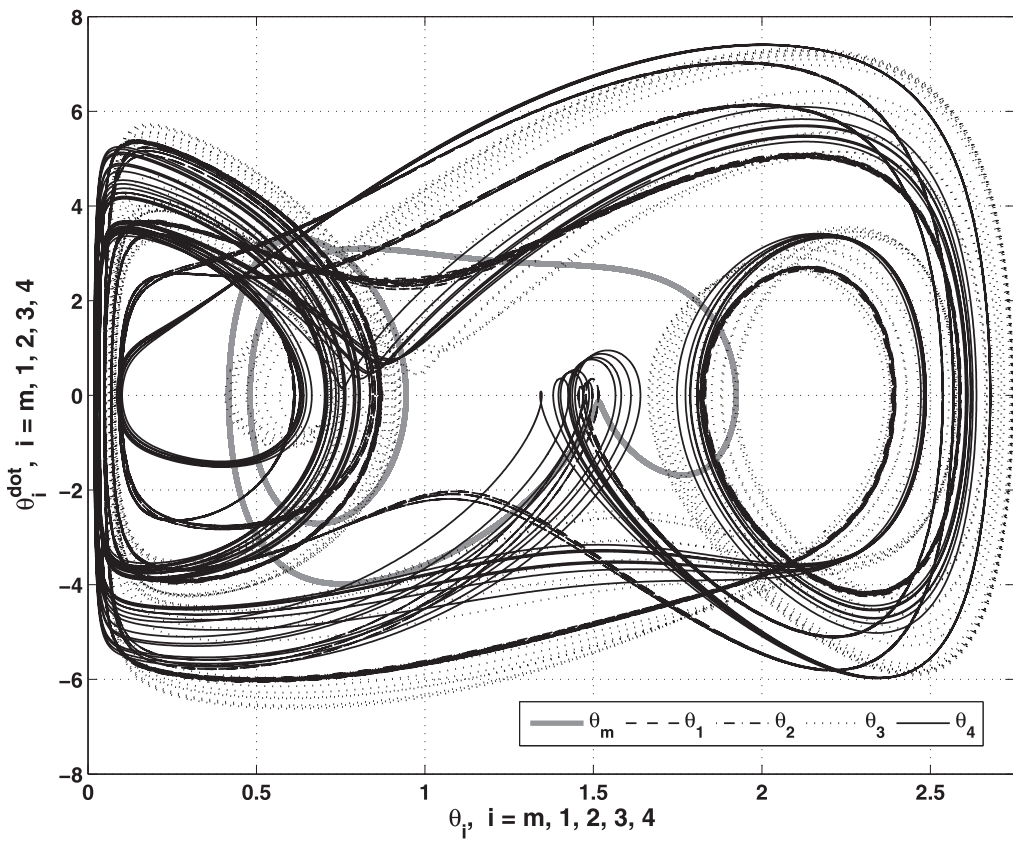


Fig. 15. Superimposed phase plot depicting the unconstrained motion of the periodic master gyro along with the four chain-coupled slave gyros for $50 \leq t \leq 100$

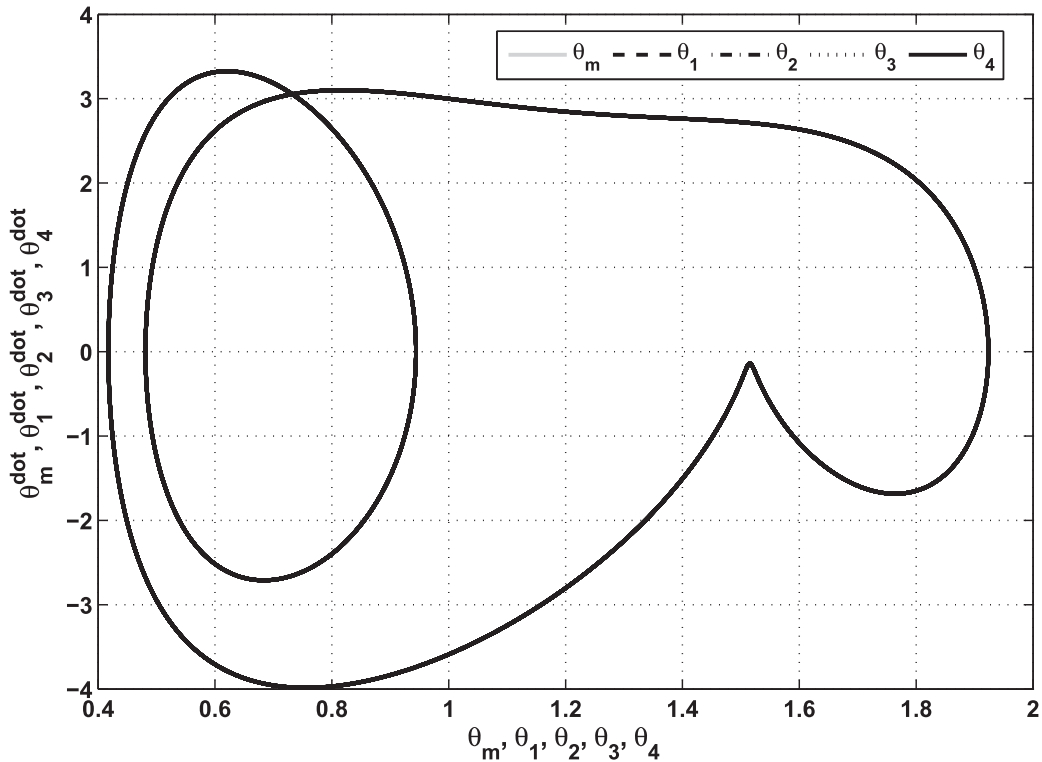


Fig. 16. A superimposed phase plot of the constrained motion of the five gyroscopes for $50 \leq t \leq 100$; the slave gyroscopes have precisely synchronized with the motion of the master gyro

behavior as expected, with their trajectories varying widely from each other. The constrained equations of motion of the master-slave system of gyroscopes are computed using Eq. (15) with the application of five constraints as described by Eq. (12). A superimposed phase plot of the constrained motion of the master-slave system of gyros is plotted in Fig. 16 for $50 \leq t \leq 100$. As can be seen from the figure, the four slave gyros (which are all chain-coupled) synchronize exactly with the periodic motion of the master gyro. The phase plot of each gyro has superimposed on top of the others, indicating precise synchronization with the master gyro. Fig. 17 shows the time history of nutation angle θ for the five gyros post-synchronization. The control torques take less than 10 s to synchronize the motion of individual slaves with that of the periodic master gyroscope. Fig. 18, on the other hand, shows the time history of synchronization errors for $60 \leq t \leq 100$. The exponential convergence of the errors to zero is evident. And finally, Fig. 19 shows a time history of the nonlinear control torques acting on the individual slave gyroscopes to obtain synchronization with the master gyro. Thus, we conclude that the removal of the sleeping condition has had little effect on the synchronization of the master-slave system of gyros.

Conclusions

In the current study, we consider the problem of synchronization of a system of n chain-coupled or general-coupled slave gyroscopes with that of a master gyroscope. However, this classical problem of tracking is approached from a constrained motion perspective. The tracking requirements are recast as constraints and the fundamental equation is used to obtain the constrained (synchronized) equations of motion of the master-slave system of gyroscopes. In the process, explicit closed form expressions for the nonlinear control torques are derived that are used to drive the system of coupled slave gyroscopes to synchronize exactly with the motion of the master gyroscope (irrespective of the chaotic or periodic behavior displayed by the master or the slave system of gyroscopes).

1. Previous investigators concern themselves with the synchronization of a set of one or two uncoupled slave gyroscopes with the motion of a master gyroscope. But the theory developed in this paper allows for a set of n slave gyroscopes that are all coupled to one another to synchronize exactly with the motion of the master gyro. Each slave gyro is a highly nonlinear

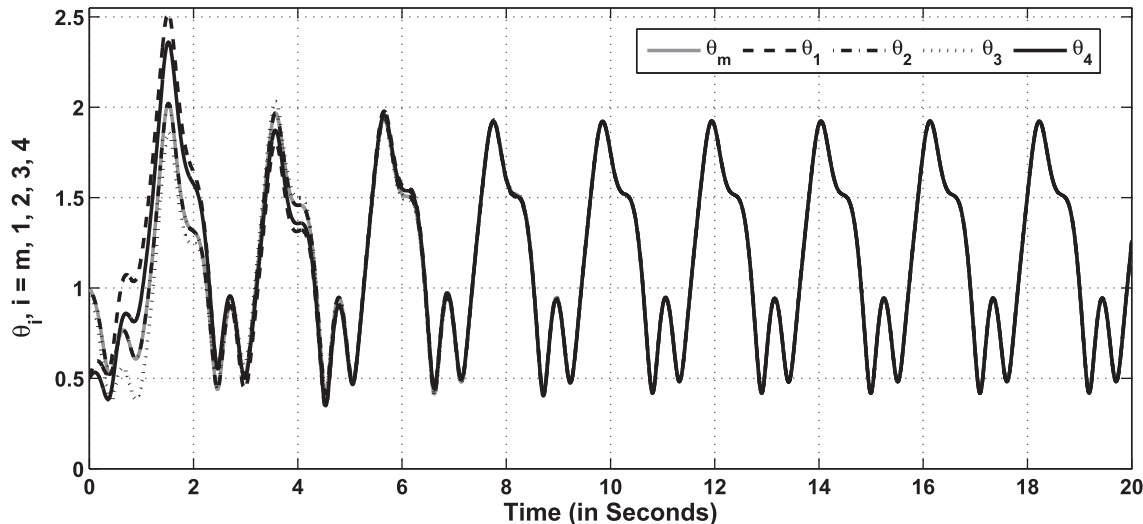


Fig. 17. Time history of θ for each individual gyroscope for $0 \leq t \leq 20$ in the constrained system

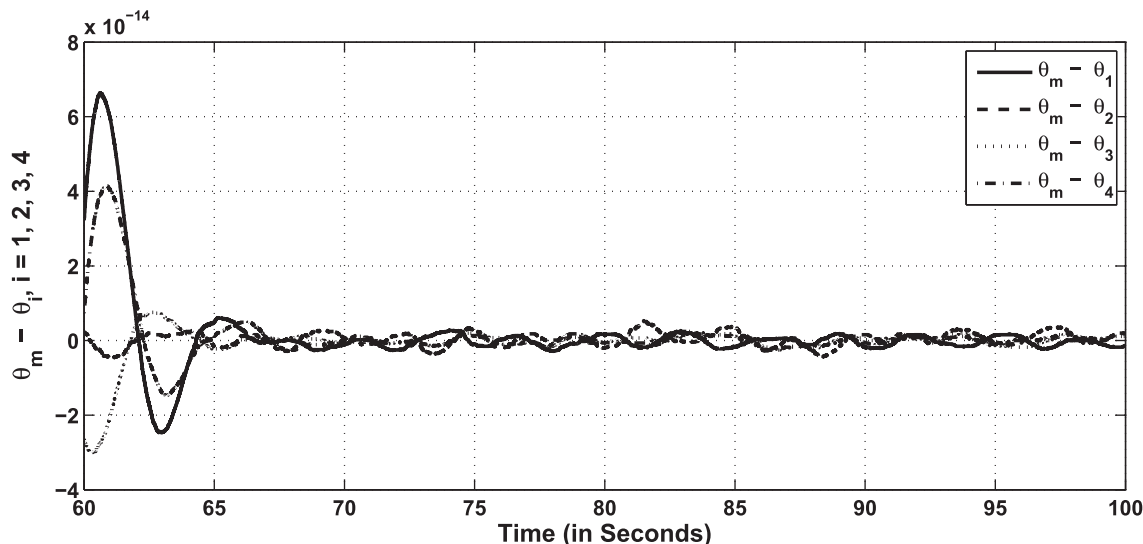


Fig. 18. Time history of synchronization errors for $60 \leq t \leq 100$; errors are smaller than the tolerance levels of the integration scheme

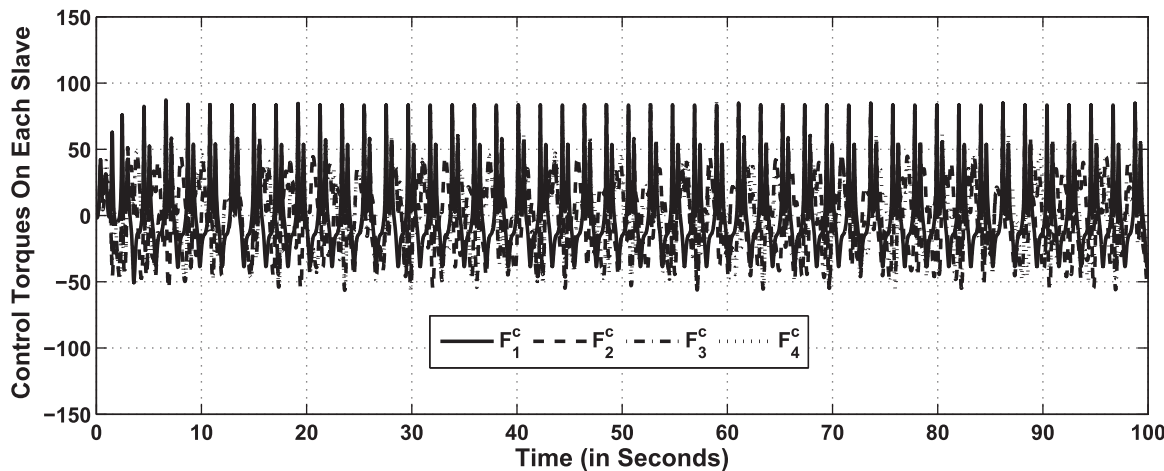


Fig. 19. Time history of the control torques acting on each individual slave gyroscope for $0 \leq t \leq 100$

- system. In addition, the slaves are nonlinearly coupled to one another with different types of couplings, and this leads to a highly nonlinear, complex dynamical system. However, the control torques are found with relative ease, showing the power and efficacy of the underlying control methods.
2. The control torques derived in this paper are continuous in time and in theory lead to exact synchronization of the master-slave system of gyroscopes. No approximations have been made in the derivation of these nonlinear control torques, or in approximating the highly nonlinear dynamics of either the master or any of the coupled slave gyroscopes.
 3. The equations of motion of a master-slave system of gyros are derived without applying the simplification of the sleeping condition. Although many authors on this subject assume the gyros to be in sleeping position, in general, most gyros do not satisfy this condition. In this paper, it is shown that removal of the sleeping condition has little effect on the synchronization of the gyroscopes as is evident from the numerical simulation.
 4. To show the efficacy of the methods presented in this paper, numerical simulations involving multiple nonidentical gyroscopes, with various types of couplings between the slave gyros, is presented. In all the cases, the control torques provided by the fundamental equation leads to an exact synchronization of the master-slave system of gyros irrespective of the chaotic or regular motions exhibited by the individual gyroscopes. It should be noted that the methods presented in this paper are applicable to any number of slave gyroscopes given any type of general, nonlinear coupling among them. The speed with which synchronization is achieved can be controlled by appropriately modifying the trajectory stabilization parameters.
 5. The constrained motion approach and the fundamental equation are powerful tools to obtain the equations of motion of constrained nonlinear mechanical systems. Thus, the methodologies provided in this paper can be readily adopted and expanded to synchronize other general nonlinear dynamical systems.

References

- Aghababa, M. P. (2011). "A novel adaptive finite-time controller for synchronizing chaotic gyros with nonlinear inputs." *Chin. Phys. B*, 20(9), 090505.
- Chen, H. K. (2002). "Chaos and chaos synchronization of a symmetric gyro with linear-plus-cubic damping." *J. Sound Vib.*, 255(4), 719–740.
- Ge, Z. M., and Chen, H. H. (1996). "Bifurcation and chaos in rate gyro with harmonic excitation." *J. Sound Vib.*, 194(1), 107–117.
- Ge, Z. M., Chen, H. K., and Chen, H. H. (1996). "The regular and chaotic motions of a symmetric heavy gyroscope with harmonic excitation." *J. Sound Vib.*, 198(2), 131–147.
- Lei, Y., Xu, W., and Zheng, H. (2005). "Synchronization of two chaotic nonlinear gyros using active control." *Phys. Lett. A*, 343(1–3), 153–158.
- Leipnik, R. B., and Newton, T. A. (1981). "Double strange attractors in rigid body motion with linear feedback control." *Phys. Lett.*, 86(A), 63–67.
- Pecora, L. M., and Carroll, T. L. (1990). "Synchronization in chaotic systems." *Phys. Rev. Lett.*, 64(8), 821–824.
- Strogatz, S. (2000). *Nonlinear dynamics and chaos*, Westview, Cambridge, MA.
- MATLAB 7.13 [Computer software]. Natick, MA, The MathWorks.
- Toda, M. (1981). *Theory of nonlinear lattices*, Springer-Verlag, Berlin.
- Tong, X., and Mrad, N. (2001). "Chaotic motion of a symmetric gyro subjected to harmonic base excitation." *J. Appl. Mech.*, 68(4), 681–684.
- Udwadia, F. E. (2003). "A new perspective on the tracking control of nonlinear structural and mechanical systems." *Proc. Royal Soc. A*, 459(2035), 1783–1800.
- Udwadia, F. E. (2000). "Nonideal constraints and Lagrangian dynamics." *J. Aerosp. Eng.*, 13(1), 17–22.
- Udwadia, F. E. (2008). "Optimal tracking control of nonlinear dynamical systems." *Proc. Royal Society A*, 464(2097), 2341–2363.
- Udwadia, F. E., and Han, B. (2008). "Synchronization of multiple chaotic gyroscopes using the fundamental equation of mechanics." *J. Appl. Mech.*, 75(2), 02011.
- Udwadia, F. E., and Kalaba, R. E. (1996a). *Analytical dynamics: A new approach*, Cambridge University Press, Cambridge, U.K.
- Udwadia, F. E., and Kalaba, R. E. (1996b). "Equations of motion for mechanical systems." *J. Aerosp. Eng.*, 9(3), 64–69.
- Udwadia, F. E., and Kalaba, R. E. (2002). "What is the general form of the explicit equations of motion for constrained mechanical systems?" *J. Appl. Mech.*, 69(3), 335–339.
- Udwadia, F. E., and von Bremen, H. (2001). "An efficient and stable approach for computation of Lyapunov characteristic exponents of continuous dynamical systems." *Appl. Math. Comput.*, 121(2–3), 219–259.
- Udwadia, F. E., and von Bremen, H. (2002). "Computation of Lyapunov characteristic exponents for continuous dynamical systems." *Z. Angew. Math. Phys.*, 53(1), 123–146.
- Udwadia, F. E., von Bremen, H., and Proskurowski, W. (2000). "A note on the computation of the largest p-Lyapunov characteristic exponents for nonlinear dynamical systems." *Appl. Math. Comput.*, 114(2–3), 205–214.
- Van Dooren, R. (2003). "Comments on chaos and chaos synchronization of a symmetric gyro with linear-plus-cubic damping." *J. Sound Vib.*, 268(3), 632–634.